China Ocean Eng., 2019, Vol. 33, No. 4, P. 385–397
DOI: 10.1007/s13344-019-0037-1, ISSN 0890-5487
http://www.chinaoceanengin.cn/ E-mail: coe@nhri.cn

Mooring System Optimisation and Effect of Different Line Design Variables on Motions of Truss Spar Platforms in Intact and Damaged Conditions

O.A. Montasir[a, *], A. Yenduri[b], V.J. Kurian[c]

[a]Department of Civil and Environmental Engineering, Universiti Teknologi PETRONAS, Seri Iskandar, Tronoh, Perak 32610, Malaysia

[b]Department of Civil Engineering, National University of Singapore, 117576, Singapore

[c]Dean of Research and Development, Providence College of Engineering, Chengannur, Alappuzha, Kerala 689122, India

Received July 16, 2018; revised February 22, 2019; accepted March 27, 2019

Abstract

This paper presents the effect of mooring diameters, fairlead slopes and pretensions on the dynamic responses of a truss spar platform in intact and damaged line conditions. The platform is modelled as a rigid body with three degrees-of-freedom and its motions are analysed in time-domain using the implicit Newmark Beta technique. The mooring restoring force-excursion relationship is evaluated using quasi-static approach. MATLAB codes *DATSpar* and QSAML, are developed to compute the dynamic responses of truss spar platform and to determine the mooring system stiffness. To eliminate the conventional trial and error approach in the mooring system design, a numerical tool is also developed and described in this paper for optimising the mooring configuration. It has a graphical user interface and includes regrouping particle swarm optimisation technique combined with *DATSpar* and *QSAML*. A case study of truss spar platform with ten mooring lines is analysed using this numerical tool. The results show that optimum mooring system design benefits the oil and gas industry to economise the project cost in terms of material, weight, structural load onto the platform as well as manpower requirements. This tool is useful especially for the preliminary design of truss spar platforms and its mooring system.

Key words: mooring optimisation, spar platform, particle swarm, Morison equation, implicit Newmark beta, quasi-static

Citation: Montasir, O.A., Yenduri, A., Kurian, V. J., 2019. Mooring system optimisation and effect of different line design variables on motions of truss spar platforms in intact and damaged conditions. China Ocean Eng., 33(4): 385–397, doi: 10.1007/s13344-019-0037-1

1 Introduction

One of the major challenges involved with the use of floating production facilities is to protect the valuable oil or gas risers from being over stressed by the platform motions. If the mooring is too flexible, then the risers need to accommodate greater deformations. If the mooring is too rigid, then the anchors in the seabed need to accommodate larger stresses. Hence, an optimal mooring configuration in terms of various line design variables will protect the platform as well as risers from extreme forces and displacements besides providing an economical design.

Recently, advanced techniques like finite element methods have been employed to evaluate the mooring line loads. However, such methods are usually adopted for the verification phase of a platform development project. The quasi-static approach is proven to be an applicable design tool for the mooring systems and is considered as a good choice for a preliminary assessment because it is almost certain to achieve convergence. If desired, a detailed assessment may further be carried out using the output from the quasi-static analysis as initial conditions for the dynamic analysis (Mavrakos et al., 1996; Smith and MacFarlane, 2001; Pascoal et al., 2005, 2006).

The spar platform is one such compliant offshore platform, which is considered as a next generation offshore structure by many oil and gas operators because of its high payload capacity and appreciable reduction of wave-induced vibrations in the range of wave frequencies (van Santen and de Werk, 1976; Glanville et al., 1991; Horton and Halkyard, 1992). Among the spar configurations mentioned, the truss spar is considered more advantageous as the cylindrical hull is shortened and thus, making the platform weigh less than classic spar which reduces the material as well as transportation cost incurred in the project (Magee et al., 2000). Therefore, the study in this paper is focused on the motion characteristics of truss spar platform.

The ratio of hull diameter to characteristic design wavelength for a typical spar platform is usually small.

*Corresponding author. E-mail: montasir.ahmedali@utp.edu.my

Hence, the wave field is virtually undisturbed by the structure and Morison equation can be assumed to be satisfactory to calculate the wave forces (Cao, 1996). The Morison equation used in combination with appreciable prediction of wave particle kinematics can give reliable platform responses for all wave frequencies (Cao, 1996). For example, the wave heights in Malaysia deep waters usually range from 0.5 m to 8 m (Yaakob et al., 2004) and are small compared with the wave length and water depths. Therefore, Linear Airy Wave Theory (LAWT) applicable for all the deep waters and considered as the most useful wave theory can be adopted to evaluate the wave kinematics (Chakrabarti, 1987).

Till date, several optimisation techniques have been developed and can be grouped into two categories depending on the search method for better positions. The first group is classified as a traditional search and second, as an artificial intelligence search. The classical methods determine the optimum solution based on the calculation of gradient, whereas the artificial intelligence methods are stochastic in nature with an extended suitability (Wang, 2012). Among various artificial intelligence approaches, the evolutionary algorithms are developed by inspiration from evolutionary paradigms and have helped to overcome most of the optimisation limitations due to their nature and strengths capitalised.

Evolutionary algorithms include Genetic Algorithm (GA) and Particle Swarm Optimisation (PSO) techniques. They serve as footstone in applying optimisation into offshore mooring design (Wang, 2012). PSO was introduced by Kennedy and Eberhart and is a heuristic algorithm inspired by artificial life in general and ties to bird flocking, fish schooling and swarming theory in particular (Kennedy and Eberhart, 1995). PSO is an extremely simple algorithm with faster convergence rate as it allows for the utilisation of prior knowledge in search process while information about local particles are shared in order to direct trajectory of swarming (Wang, 2012) and slightly more accurate than GA (Kennedy and Eberhart, 1995; Hassan et al., 2005; Shi and Eberhart, 1998; Hu et al., 2003; Albrecht, 2005). PSO has been found to be successful in many engineering applications like composite beam design (Kathiravan and Ganguli, 2007), logic circuits design (Coello et al., 2003), control design (Zheng et al., 2003; Krohling et al., 2003), concrete beam design (McCluskey, 2008), offshore mooring design (Albrecht, 2005; Monteiro et al., 2010), etc. Based on the results presented by Monteiro et al. (2010), the application of optimization using evolutionary algorithms, especially PSO in offshore mooring systems is effective and robust as it can also bring greater security to the designer in obtaining appropriate values for platform offsets and mooring lines tractions.

A study on the effect of mooring line azimuth angles has been presented by Montasir et al. (2015, 2016). The primary objective of this study is to investigate the dynamic responses of the truss spar platforms in intact and damaged line conditions for mooring design variables, viz., line diameters, fairlead slopes and pretensions. The second objective is to develop an efficient numerical tool using particle swarm optimisation technique (PSO) to predict the optimum mooring configuration of a given truss spar platform in a shorter duration compared with the conventional trial and error approach.

2 Numerical modelling

2.1 Hydrodynamics of truss spar platform

One of the useful theories in calculating the progressive wave kinematics is linear Airy wave theory. It is based on the assumption that the wave height is small compared with the wave length. This assumption allows the free surface boundary conditions to be linearized by dropping wave height terms which are beyond the first order. These conditions are also to be satisfied at the mean water level rather than at the oscillating free surface. The governing equations for the wave kinematics using the linear Airy wave theory and wave forces using the modified Morison equation (relative velocity model) are as detailed in Montasir et al. (2016).

Let $\boldsymbol{M}$, $\boldsymbol{C}$, $\boldsymbol{K}$, and $\boldsymbol{F}$ be the structural mass, damping, stiffness and resultant force matrices respectively, $\ddot{\boldsymbol{P}}$, $\dot{\boldsymbol{P}}$ and $\boldsymbol{P}$ be the structure acceleration, velocity and displacement matrix, then the equilibrium equation is given in Eq. (1) as:

$$\boldsymbol{M}\ddot{\boldsymbol{P}}+\boldsymbol{C}\dot{\boldsymbol{P}}+\boldsymbol{K}\boldsymbol{P}=\boldsymbol{F}. \tag{1}$$

The mass, damping, stiffness and force matrices are as detailed in Montasir et al. (2016). The response analysis is performed in time-domain using implicit Newmark Beta method. Montasir et al. (2016) shows the flowchart of the implicit Newmark Beta procedure. Once the computation is started, the dynamic equilibrium can be checked by evaluating the dynamic-out-of-balance force. If the unbalanced force is less than the specified error, the equilibrium is attained and the procedure progresses to the next time-step. If otherwise, an iterative process within each time-step begins in order to eliminate this unbalance force.

A numerical code named *DATSpar* has been developed to compute the dynamic responses of the truss spar platform using the above described numerical modelling.

2.2 Mooring line restoring forces

The analysis has been carried out for the mooring line with disturbed clump weight by referring to the flowchart as depicted in Montasir et al. (2016) and according to the analysis procedure given in Agarwal and Jain (2003); incorporating the two conditions mentioned for the clump weight lift-off from the seabed.

A numerical code named *QSAML* has been developed to compute the restoring forces of the mooring system using

the above described quasi-static approach.

2.3 Optimisation numerical tool – *MoorOpt14*

The workflow and user interface of the software tool – *MoorOpt14* to predict the optimum mooring configuration of truss spar platform are as depicted in Figs. 1 and 2, respectively. This tool is an integration of three numerical codes viz. PSO code, *DATSpar* and *QSAML*.

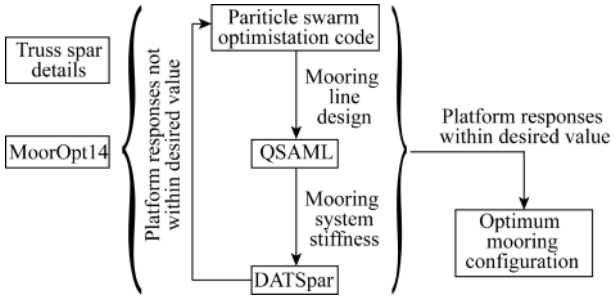

Fig. 1. Workflow of *MoorOpt14*.

MoorOpt14 is developed to optimise the mooring configuration of truss spar platforms in terms of line azimuth angles, line diameter, line fairlead slope and line pretension. Two numerical codes named *DATSpar* and *QSAML* are developed for computing the dynamic responses of truss spar platforms and mooring system restoring forces, respectively. They are validated using model tests results given in the literature (Technip document, 2005; Ran, 2000). The two codes are then used for investigating the effect of various mooring line design variables i.e. azimuth angles, diameter, fairlead slope, grouping, material and pretension on the dynamic responses of truss spar platforms in intact and damaged line conditions to predict the criteria for obtaining optimum mooring configuration of truss spar platforms. The criteria developed from various mooring line design variables studied are input to this tool as their preferred range of values to obtain an optimised mooring configuration for the truss spar platforms. To demonstrate the functioning of this tool, a case study is presented on an existing truss spar platform.

2.3.1 *PSO technique*

PSO is based on the population of random solutions called particles. Every particle has a velocity that allows them to search throughout the domain. The velocity vector gets updated using the historical behaviour of particles i.e. particles best position. The position x of a particle i at time t is updated as given in Eq. (2).

$$x_t^i = x_{t-1}^i + v_t^i \Delta t. \tag{2}$$

The incremental step Δt is taken as unity in this study for convenience of calculation. All the particles set values for each input design variable which are defined as the dimensions of solution space. The velocity component of a particle is separated into vectors having multi-dimensions. Each dimension in velocity represents changing of a variable. The velocity vector of a particle can be calculated by Eq. (3).

$$v_t^i = w_{\text{in}} v_{t-1}^i + \frac{c_1 r_1 \left(p_{t-1}^i - x_{t-1}^i\right)}{\Delta t} + \frac{c_2 r_2 \left(p_{t-1}^g - x_{t-1}^i\right)}{\Delta t}, \tag{3}$$

where, r_1 and r_2 are generated uniformly between 0 and 1 for the purpose of providing randomness, c_1 and c_2 are called acceleration coefficients and are parameters showing the confidence particle in itself and among the swarm respectively.

The coefficient of inertia w_{in}, also called as inertia weight is introduced to improve PSO performance. Appropriate selection of inertia weight provides a good balance between global and local exploration (Al-geelani et al., 2013). The inertia weight w_{in} can be set as per Eq. (4).

$$w_{\text{in}} = w_{\max} - \frac{w_{\max} - w_{\min}}{iter_{\max}} \times t, \tag{4}$$

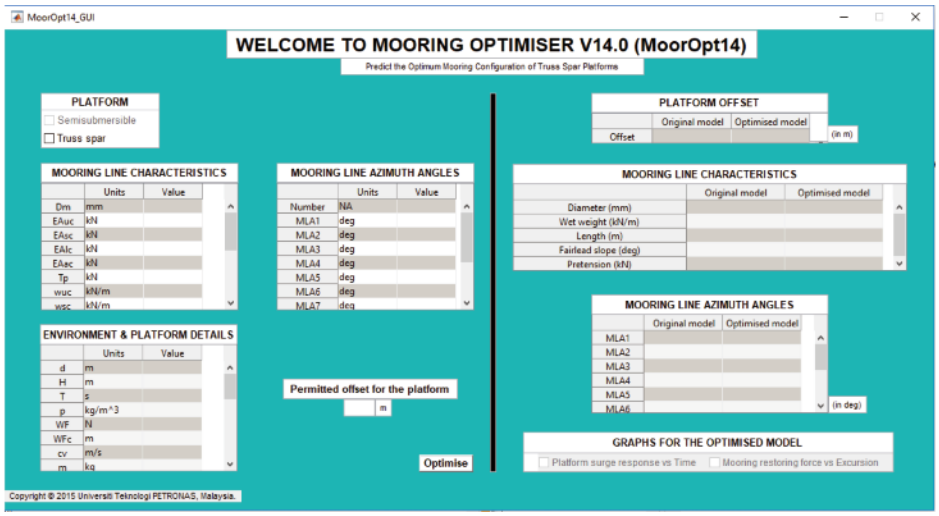

Fig. 2. Graphical user interface of *MoorOpt14*.

The pseudo code for PSO is as follows (Wang, 2012):

```
WHILE stopping criteria reached
 FOR each particle, calculate fitness value based on objective function
  FIND the velocities for each particle
  IF the fitness value is better than best fitness memorised in history
   SET 1. the best fitness value to current better value and stored
       2. new particle positions
  END
 END
END
```

2.3.2 *PSO Parameters*

PSO is influenced by many control parameters namely the dimension of a problem, number of particles, acceleration coefficients, inertia weight, number of iterations and if velocity clamping is used to avoid the phenomenon of swarm explosion, then the maximum velocity also influences the performance of PSO.

Larger number of particles explore greater response surface at each iteration and hence, will have a higher possibility to find the global minimum. However, excessive size of swarm can result in parallel random search and thus, increasing the computational time. A swarm size of 10 to 30 is found to be appropriate from empirical studies (Brits et al., 2002; Van den Bergh and Engelbrecht, 2001). Nevertheless, the best swarm size depends on optimisation problem as this size is found based on trial and error (Wang, 2012).

The acceleration coefficients control the random search of cognitive and social components of velocity. A larger coefficient makes the particles wander excessively, while a smaller coefficient tends to trap the optimisation in local minima. The inertia weight and acceleration coefficients can be claimed to be stable as long as the below mentioned criteria in Eq. (5) is satisfied.

$$0 < c_1 + c_2 < 4 \text{ and } \left(\frac{c_1 + c_2}{2} - 1\right) < w < 1. \tag{5}$$

When running the PSO, it can be noted that sometimes there is a set of iterations that show no improvement. However, early termination may result in sub-optimal solution and late termination can take extra computational time. Hence, the stopping criteria includes (Wang, 2012):

(1) The number of iterations specified by user.

(2) The value of an objective function is not improving over a certain number of iterations.

(3) A certain proportion of particles are clustered (Van den Bergh and Engelbrecht, 2001).

The PSO parameters settings used in this study are shown in Table 1.

The velocity clamping effect was introduced to avoid the phenomenon of swarm explosion. With no restriction on the maximum velocity of particles, a one-dimensional analysis concludes that the particle velocity can be unbounded while the particle oscillates around an optimum, increasing its distance to the optimum on each iteration. When compared with other evolutionary computation techniques, PSO quickly identifies the region where optimum is located but only has a trouble to adjust the velocity to lower values to perform a fine search of solution space (Al-geelani et al., 2013). The best results can be achieved when both velocity clamping and constriction mechanisms are combined using *Vmax* equal to *Xmax* faster convergence rates can be obtained (Eberhart and Shi, 2000).

Table 1 Parameters settings for PSO in this study

Parameter	Value
Dimension of problem	7
Number of particles	5
c_1, c_2	1.49618
Inertia weight	[0.9, 0.4]
Number of iterations per grouping	10
Velocity clamping percentage	0.50

2.3.3 *Regrouping*

Swarm escape from the state of premature convergence is often troublesome in nonlinear problems. Here the regrouping mechanism makes use of swarm state and reorganizes it according to information inferred i.e. more than just restarting on the same search space repeatedly. Regrouping mechanism developed by (Evers, 2009) was able to solve the stagnation problem and approximate the true global minimizer with each trial conducted. Hence, the same mechanism is incorporated along with PSO in this study.

3 Validation of numerical predictions

3.1 Dynamic responses of truss spar platform and mooring line restoring force

A MATLAB code named DATSpar has been developed to compute the dynamic responses of the truss spar platform subjected to unidirectional regular waves, steady current and wind loadings. The numerical code is validated with experimental measurements from literature (Technip document, 2005) for the truss spar platform mentioned in Montasir et al. (2016).

To compute restoring forces in mooring lines, quasi-static approach is adopted for the analysis and a MATLAB code named QSAML has been developed. The numerical code is validated with experiment measurements from literature (Ran, 2000) by comparing the mooring stiffness curve obtained for the MARLIN truss spar mooring configuration mentioned in Montasir et al. (2016).

3.2 Functioning of PSO

The functioning of optimisation method involved in this tool i.e. PSO with regrouping mechanism is checked using five mathematical benchmark functions viz. Ackey, Griewangk, Rastringin, Rosenbrock and Sphere as summarised in Table 2. These five functions are considered to be good benchmark functions for an optimising program be-

Table 2 Benchmark functions for checking the functioning of PSO

Function name	Function	Dimension	Initial range of x_i
Ackley	$f(x)=-20\exp\left(-0.2\sqrt{\frac{1}{n}\sum_1^n x_i^2}\right)-\exp\left[\frac{1}{n}\sum_1^n\cos(2\Pi x_i)\right]+20+\exp(1)$	10	[–30, 30]
Griewangk	$f(x)=\frac{1}{40000}\sum_1^n x^2-\Pi_1^n\cos\left(\frac{x_i}{\sqrt{i}}\right)+1$	10	[–600, 600]
Rastringin	$f(x)=10n+\sum_1^n x_i^2-10\cos(2\Pi x_i)$	10	[–5.12, 5.12]
Rosenbrock	$f(x)=\sum_1^{n-1}\left[100\left(x_{i+1}-x_i^2\right)^2+(1-x_i)^2\right]$	10	[–2.048, 2.048]
Sphere	$f(x)=\sum_1^n x_i^2$	10	[–5.12, 5.12]

cause they include several local minima with only one global minimum viz. Griewangk's function, and Sphere function are uni-modal and Ackey's function, Rastringin's function, Rosenbrock's function are multi-modal (Wang, 2012). The graphs of these benchmarking functions are shown in Figs. 3 and 4.

The quantity of local minima increases exponentially with dimensionality. The dimensionality for all the benchmark functions is chosen as ten. The use of high dimensionality is due to the nature of mooring configuration optimisation problems whose dimensionality is associated with the number of line variables and usually is less than ten (Wang, 2012). Therefore, benchmarking the five functions in a ten dimensionality space is considered to be appropriate.

4 Mooring line characteristics

The two codes – *QSAML* and *DATSpar*, after validation are used to investigate the dynamic responses of truss spar platform for different mooring line design variables. A floating platform with fairleads at 941.832 m (Ran, 2000) from the seabed is considered for the present study. The other particulars of this platform are as considered for the validation study. The platform is stationed with nine mooring lines and the azimuth angles are as considered for the validation study.

The mean position of platform is determined for a high frequency wave (time period used is 4 s) which can cause a relatively large initial offset due to its high energy, wave height of 6 m, steady current of 1.34 m/s and wind load of 237 kN. These wave height, current and wind load values are for a deep water location in Malaysia and are taken from (Technip document, 2005). The damaged mooring conditions are generated by removing one line from group-I as lines in this group are the most tensioned. The characteristics of all mooring line components in the different design variable studies are described in Section 6 (original model), except where specified.

The diameters of mooring lines for any floating platform usually range from 4″ to 5″ and slightly greater for very few cases. Hence, the study is conducted by choosing mooring line diameters ranging from 3″ to 6″ (i.e. 76.2 mm

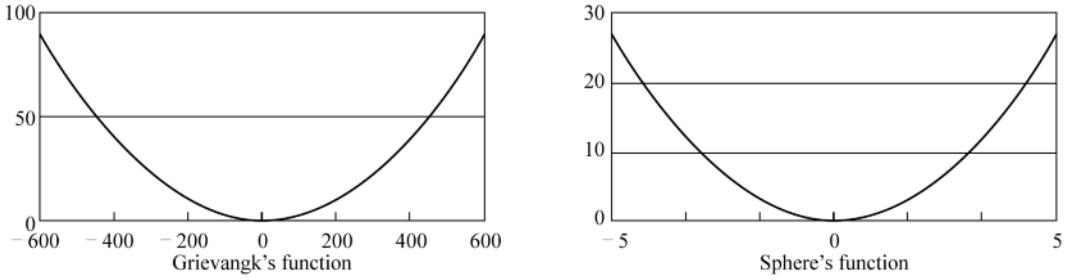

Fig. 3. Graphs of uni-modal benchmark functions (Wang, 2012).

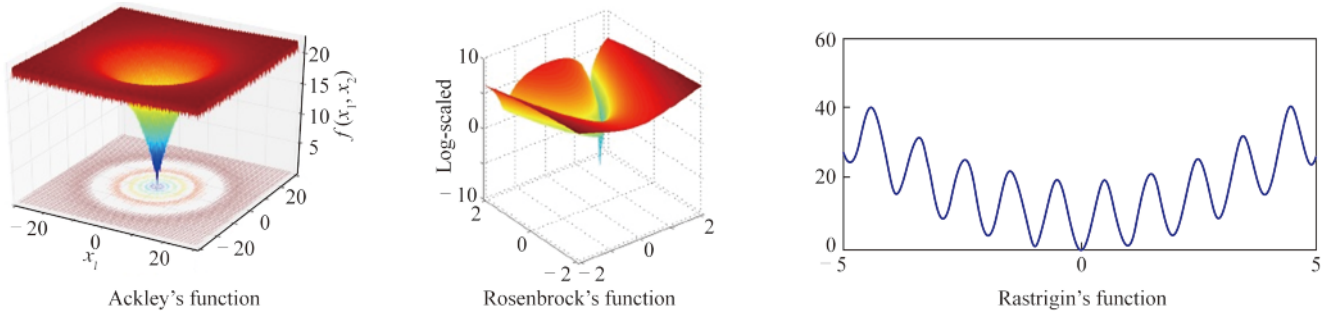

Fig. 4. Graphs of multi-modal benchmark functions (Wang, 2012).

to 152.4 mm). The characteristics of mooring line middle component for various diameters chosen are given in Table 3.

Table 3 Characteristics of mooring line for different diameters

S. No.	Diameter (mm)	Wet weight (kN/m)	Effective modulus (kN)	Breaking load (kN)
1	76.2	0.2986	911598	4005
2	82.6	0.3506	1069863	4693
3	88.0	0.3986	1215793	5326
4	95.3	0.4673	1424376	6231
5	101.6	0.5319	1620625	7082
6	108.0	0.6007	1829535	7987
7	114.3	0.6737	2051106	8947
8	120.7	0.7508	2285338	9960
9	127.0	0.8322	2532232	11029
10	133.4	0.9177	2791786	12152
11	139.7	1.0074	3064002	13329
12	146.1	1.1013	3348880	14560
13	152.4	1.1994	3646418	15846

The study on fairlead slopes is conducted by varying the top slopes of mooring lines from 45° to 65°. The change in mooring line length for different slopes is incorporated only in middle component keeping the lengths of top and lower component unchanged. Table 4 gives the lengths of mooring line middle component for various fairlead slopes chosen.

Table 4 Characteristics of mooring line for different fairlead slopes

Fairlead slope (°)	Length of mooring line middle component (m)
45.8	2250
50.3	1500
56.6	1200
59.4	1100
64.1	1000

The study on mooring line pretensions is conducted with 25 values ranging from 1.8×10^3 kN to 5.0×10^3 kN. All the nine mooring lines are modelled with same pretension values.

5 Case study to demonstrate the efficiency of *MoorOpt14*

The efficiency of *MoorOpt14* is presented by a case study comparing the mooring configurations of original and optimised models i.e. in terms of line azimuth angles, line diameter, line fairlead slope (line length) and line pretension. The original mooring line design variables for the platform are shown in Tables 5 and 6.

Table 5 Characteristics of the truss spar mooring lines – Original model

Legend	Parameters							
	Type	Length (m)	Fairlead slope	Diameter (mm)	Wet weight (kN/m)	Effective Modulus (kN)	Breaking load (kN)	Pretension (kN)
Top component	Chain cable	76.2		–	2.73	665852	13188	2.312×10^3
Middle component	Steel wire/cable	1828.7	–	108.0	0.6007	1829535	7987	–
Lower component	Chain cable	45.7	–	–	2.73	858882	13188	–

Table 6 Truss spar mooring lines azimuth angles – Original model (Azimuth angles are mentioned with respect to *wave heading South*)

Group	Mooring lines azimuth angles
I	45°, 50°
II	125°, 132.5°
III	222.3°, 229.7°, 235°
IV	308.5°, 314.1°, 320.3°

The optimum mooring configuration of truss spar platform is determined by considering the following constraints:

(1) Offset of platform should be minimum (threshold value is assumed to be 4 m).

(2) Mooring line diameter, length (defined in terms of fairlead slopes) and pretension should be minimum.

(3) Mooring line tension should be limited to 0.5 and 0.7 times breaking load in intact and damaged line conditions respectively as per American Petroleum Institute (2005).

Based on the inferences obtained from mooring line design variables studies (Azimuth angles - Montasir et al., 2015 and Montasir et al., 2016; Diameters, Fairlead slopes and Pretensions – Current paper), the range of values mentioned in Tables 7 and 8 are input as initial line characteristics and azimuth angles into *MoorOpt14* to optimise the mooring system configuration of truss spar platform.

6 Results and discussions

6.1 Validation of QSAML and DATSpar

The comparison of mooring system restoring forces obtained from numerical code *QSAML* and RAOs predicted by

Table 7 Initial mooring line characteristics considered for optimisation

Legend	Parameters			
	Type	Diameter (mm)	Fairlead slope	Pretension (kN)
Top component	Chain cable	–	50° to 65°	1.8×10^3 to 3.0×10^3
Middle component	Steel wire/cable	75 to 115	–	–
Lower component	Chain cable	–	–	–

Table 8 Initial mooring line azimuth angles considered for optimisation(Azimuth angles are mentioned with respect to *wave heading South*)

Group	Azimuth angle for one mooring line in the group	Remarks
Ⅰ (2 lines)	0° to 30°	All the other lines in each group differ by +5° for two lines group and +5°, +10° for three lines group
Ⅱ (2 lines)	90° to 120°	
Ⅲ (3 lines)	180° to 210°	
Ⅳ (3 lines)	270° to 300°	

DATSpar with experimental measurements is given in Montasir et al. (2015).

6.2 Restoring behaviour of the mooring system for different line diameters

Fig. 5 shows the restoring behaviour of mooring system for line diameters ranging from 82.6 to 133.4 mm (Note: Behaviours with other line diameters are not shown in the figure to avoid congestion between the curves). It can be observed that the restoring performance in intact condition decreases as the line diameter increases. This can be attributed to the increase in wet weight of mooring line with diameter and thus, causing the reduction in line tensions leading to decrease in the restoring forces. It can also be observed that the difference in mooring restoring performance and maximum permissible excursions increase with line diameters.

From Fig. 5, it can also be observed that the effect of damaged mooring line on restoring performance is significant for all diameters. The reduction in mooring restoring forces in damaged condition decreases for higher line diameters. In case of mooring line failure, the maximum difference in restoring forces for line diameters 82.6 to 133.4 mm range from 57.14% to 36.36%, respectively.

6.3 Dynamic motions of platform for different mooring line diameters

Figs. 6 and 7 show the motions of platform in about its mean position for three mooring diameters i.e. 76.2 mm,

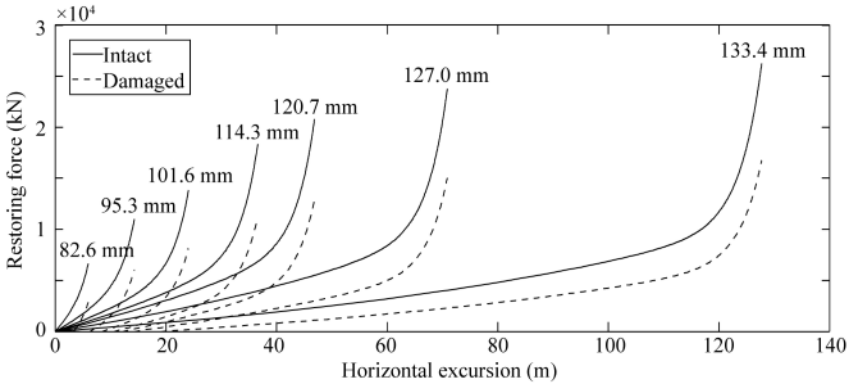

Fig. 5. Mooring system restoring behaviour for different diameters – intact and damaged line conditions.

Fig. 6. Surge and pitch RAOs of the platform for different mooring diameters – intact line condition.

Fig. 7. Surge and pitch RAOs of the platform for different mooring diameters – damaged line condition.

101.6 mm and 136.7 mm in intact and damaged conditions (Note: Behaviours with other line diameters are not shown in the figure to avoid congestion between the curves). It can be observed that in general, the performance of mooring system for three line diameters in terms of the motions of platform at its mean position is nearly the same i.e. the difference in surge as well as pitch RAOs is insignificant and absolutely zero in the heave RAOs. It can also be observed that the variation in surge and pitch RAOs between intact and damaged line conditions is insignificant for all wave periods.

Fig. 8 shows the mean positions of platform for different mooring line diameters. It can be observed that the mean position attained by platform in intact condition increases as the line diameter increases. It can be inferred that relatively higher increase in mean position starts from 127.0 mm line diameter ranging from 10.27 to 86.21 m. This can be attributed to the decrease in restoring performance with increase in line diameter as depicted in Fig. 5.

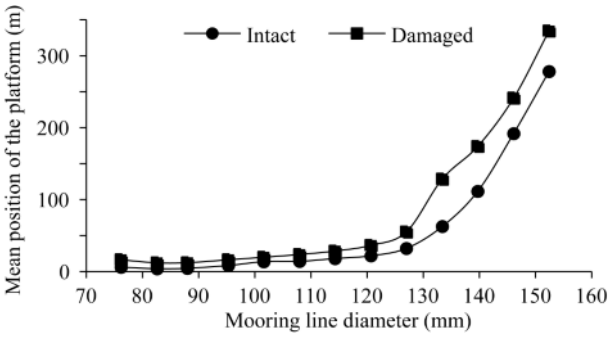

Fig. 8. Mean position of the platform for different mooring diameters – intact and damaged conditions.

From Fig. 8, it can also be observed that the effect of damaged mooring line on mean position of platform is significant for all diameters. In case of mooring line failure, the variation in mean position of platform is 6.29 to 9.57 m for diameters ranging from 76.2 to 114.3 mm. The variation in mean position is 14.59 to 56.42 m for diameters ranging from 120.7 to 152.4 mm. Therefore, it can be inferred that the variation in mean position of platform for diameters ranging from 120.7 to 152.4 mm is higher than the variation in mean position of platform for diameters ranging from 76.2 to 114.3 mm.

6.4 Restoring behaviour of the mooring system for different line fairlead slopes

Fig. 9 shows the restoring behaviour of mooring system for different line fairlead slopes. It can be observed that the mooring restoring performance in intact condition increases as the fairlead slope increases. The restoring performance is greatly enhanced when line fairlead slope is changed from 45.8° to 50.8° and beyond. It can also be observed that the maximum permissible horizontal excursion of mooring system decreases as the fairlead slope increases.

From Fig. 9, it can also be observed that the effect of damaged mooring line on restoring performance is significant for all fairlead slopes. The reduction in mooring restoring forces in damaged condition increases with fairlead slope. In case of mooring line failure, the maximum difference in restoring forces for fairlead slopes 45.8° to 64.1° ranges from 35.71% to 38.46%, respectively.

6.5 Dynamic motions of platform for different mooring line fairlead slopes

Figs. 10 and 11 show the motions of platform in about its mean position for different mooring fairlead slopes in intact and damaged conditions. It can be observed that in general, the performance of mooring system for all line fairlead slopes in terms of the motions of platform at its mean position is nearly the same i.e. the difference in surge as well as pitch RAOs is insignificant and absolutely zero in the heave RAOs. It can also be observed that the variation in surge and pitch RAOs between intact and damaged line conditions is insignificant for all wave periods.

Fig. 12 shows the mean positions of platform for differ-

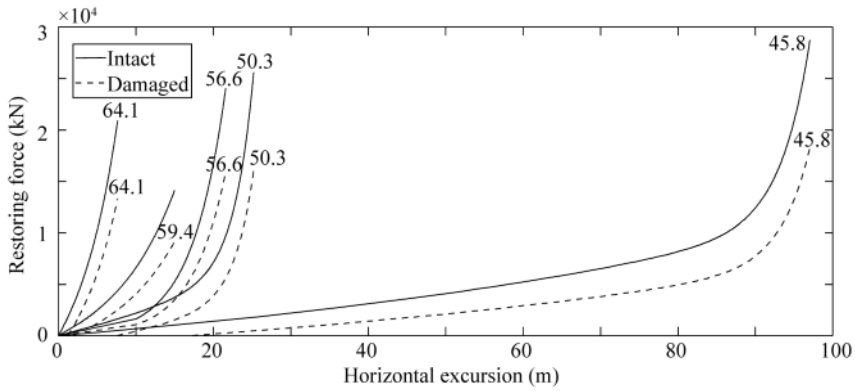

Fig. 9. Mooring system restoring behaviour for different fairlead slopes – intact and damaged line conditions (Line fairlead slopes mentioned in the figure are in degrees).

Fig. 10. Surge and pitch RAOs of the platform for different mooring fairlead slopes – intact line condition.

Fig. 11. Surge and pitch RAOs of the platform for different mooring fairlead slopes – damaged line condition.

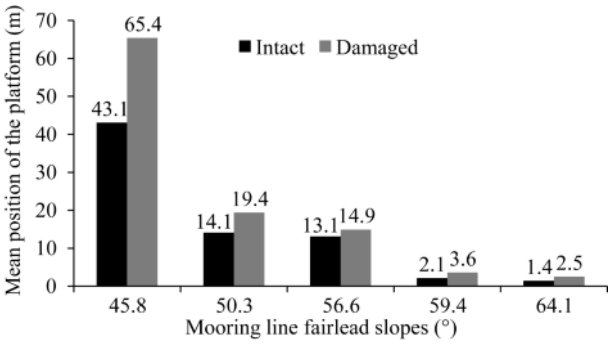

Fig. 12. Mean position of the platform for different mooring fairlead slopes – intact and damaged conditions.

ent mooring line fairlead slopes. It can be observed that the mean position attained by platform in intact condition decreases as the line fairlead slope increases and can be attributed to the increase in restoring performance as depicted in Fig. 9. Similar to difference in mooring restoring performance, the mean position of platform is drastically reduced when line fairlead slope changes from 45.8° to 50.8° and beyond.

From Fig. 12, it can also be observed that the mean position of platform is affected when mooring line is damaged. The variation in mean position of platform ranges from 22.3 m to 1.1 m for mooring line fairlead slopes from 45.8° to 64.1° respectively. In case of mooring line failure, the variation in mean position of platform is 5.3 m to 1.1 m for fairlead slopes ranging from 50.3° to 64.1° respectively but relatively higher variation of 22.3 m in mean position is observed for fairlead slope 45.8°.

6.6 Restoring behaviour of the mooring system for different line pretensions

Fig. 13 shows the restoring behaviour of mooring system for line pretensions ranging from 1.8×10^3 kN to 4.0×10^3 kN (Note: Behaviours with other line pretensions are not shown in the figure to avoid congestion between the curves). It can be observed that the restoring performance in intact condition increases as the line pretension increases. It can also be observed that the difference in mooring restoring performance and maximum permissible excursions decreases as the line pretension increases. This variation is more obvious between line pretensions 1.8×10^3 kN to 2.2×10^3 kN, relatively less from 2.2×10^3 kN to 3.0×10^3 kN and even lesser beyond 3.0×10^3 kN.

From Fig. 13, it can also be observed that the effect of damaged mooring line on restoring performance is significant for all pretensions. The reduction in mooring restoring forces in damaged condition increases for higher line pretensions. In case of mooring line failure, the maximum difference in restoring forces for line pretensions 1.8×10^3 kN to 4.0×10^3 kN ranges from 41.16% to 40.77%, respectively.

6.7 Dynamic motions of platform for different mooring line pretensions

Figs. 14 and 15 show the surge and pitch motions of platform in intact and damaged line conditions for four mooring pretensions (Note: RAOs with other line pretensions are not shown in the figure to avoid congestion between the curves). In general, it can be observed that the performance of mooring system for four line pretensions in terms of the motions of platform at its mean position is nearly same i.e. the difference in surge and pitch RAOs is

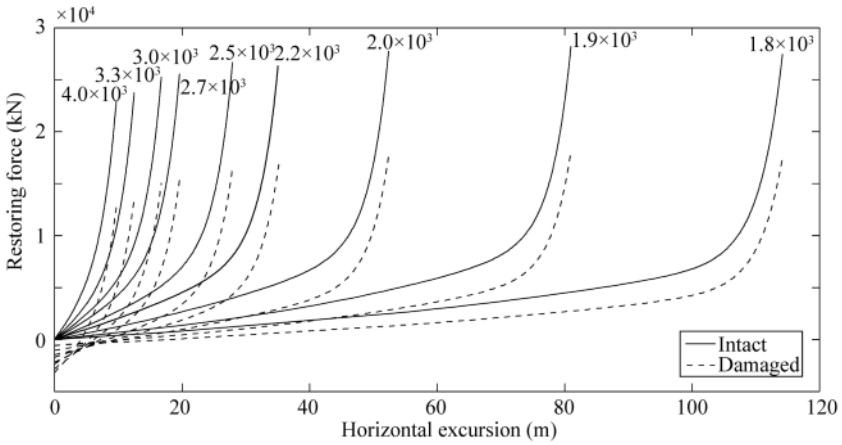

Fig. 13. Mooring system restoring behaviour for different pretensions – intact and damaged line conditions (Line pretensions mentioned in the figure are in kN).

Fig. 14. Surge and pitch RAOs of the platform for different mooring pretensions – intact line condition (Line pretensions mentioned in figure are in kN).

Fig. 15. Surge and pitch RAOs of the platform for different mooring pretensions – damaged line condition (Line pretensions mentioned in figure are in kN).

insignificant and absolutely zero in heave RAOs. It can also be observed that the variation in surge and pitch RAOs between intact and damaged line conditions is insignificant for all wave periods.

Fig. 16 shows the mean positions of platform for different mooring line pretensions. It can be observed that the mean position attained by platform in intact condition decreases as the line pretension increases and can be attributed to the increase in restoring performance. It can be inferred that relatively higher mean positions are obtained from 1.8×10^3 kN to 3.0×10^3 kN line pretensions ranging from 70.75 m to 5.01 m respectively and thereafter, is nearly the same. This can be attributed to the decrease in restoring performance variations with increase in line pretension as depicted in Fig. 13.

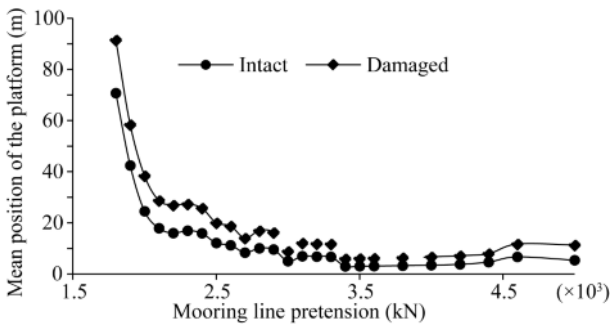

Fig. 16. Mean position of the platform for different mooring pretensions – intact and damaged conditions.

From Fig. 16, it can also be observed that the effect of damaged mooring line on mean position of platform is sig-

nificant for all pretensions. In case of mooring line failure, the variation in mean position of platform is 20.79 m to 3.84 m for pretensions ranging from 1.8×10^3 kN to 3.0×10^3 kN respectively but thereafter, smaller variation is observed in mean position which is nearly 1.65%.

6.8 Functioning of PSO

Fig. 17 shows the global minima and global-best patterns obtained by regrouping PSO for five benchmark functions viz. Ackley, Griewangk, Rastringin, Rosenbrock and Sphere considered to study its functioning.

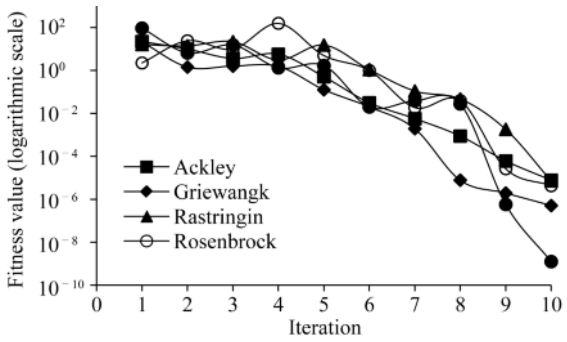

Fig. 17. Functionality of PSO for five benchmark functions.

The global minima of the five mathematical functions are as given by $f(x)$ in Table 2. It can be observed that the regrouping PSO can minimise the Ackley, Rastringin and Rosenbrock mathematical functions to nearly 10^{-6}, Griewangk mathematical function to nearly 10^{-7} and Sphere mathematical function to nearly 10^{-9}. It can be inferred that the percentage of error for regrouping PSO to find global minima is smaller than 0.1%. Therefore, a combination of final results shown in Table 9 indicates that regrouping PSO is capable of finding the near optimum solutions.

6.9 Case study – *MoorOpt14*

The optimised mooring configuration of truss spar platform obtained from *MoorOpt14* is presented in Tables 10, 11, 12 and Fig. 18. These tables show the comparison of platform offset (mean position) and mooring line design variables values for original and optimised models.

It can be observed that the platform offset is reduced from 11.389 m to 3.136 m against the preferred value of 4 m. The reduction in mooring line diameter leading to 15.98% of decrease in wet weight and the reduction in mooring line length by 24.45%, decreases the structural load on hull by an amount of 401.207 kN (i.e. $0.6007\times1828.7 - 0.5047\times1381.6 = 401.207$ kN) due to each line. The reduction in mooring line pretension by 13.04%, decreases the structural load on hull by an amount of 301.6 kN (i.e. $2.312\times10^3 - 2.0104\times10^3 = 301.6$ kN) due to each line. Therefore, 7028.07 kN of the structural load on hull from all mooring lines and 4477 m of line length in total are reduced leading to an economical design of truss spar platform.

It should be mentioned here that the optimisation of mooring line design variables for this case study is performed on a 3rd generation Intel Core i5 CPU @ 2.50GHz and the duration was 35 minutes.

7 Conclusions

The main finding from this study is that the effect of the mooring diameters, fairlead slopes and pretensions on the motions of truss spar platform about its new mean position is insignificant in all line conditions. However, the mean position of the platform besides mooring system restoring performance is significantly affected. In addition, the presented tool – *MoorOpt14* is able to optimise the mooring configuration of a truss spar platform subjected to wave, current and wind environmental loadings by keeping the platform displacements in an adequate range, while not exceeding the line tension criteria.

The following are the specific conclusions drawn, based on the numerical study conducted.

(1) For both intact and damaged mooring conditions, the restoring performance decreases with increase in line diameter and increases as line fairlead slope/line pretension increases.

(2) In case of mooring failure, the maximum reduction in restoring forces decreases as line diameter increases and increases with line fairlead slope/line pretension.

Table 9 Benchmark function results obtained using PSO

Variables	Ackley	Griewangk	Rastringin	Rosenbrock	Sphere
x_1	-4.49×10^{-6}	3.07×10^{-4}	-1.38×10^{-8}	0.9999941	1.170×10^{-5}
x_2	-1.13×10^{-6}	-3.72×10^{-4}	4.22×10^{-8}	0.9999922	1.170×10^{-5}
x_3	-1.84×10^{-6}	-0.96×10^{-4}	1.77×10^{-6}	0.9999800	1.168×10^{-5}
x_4	1.31×10^{-6}	-3.12×10^{-4}	-1.03×10^{-6}	0.9999551	1.166×10^{-5}
x_5	-1.51×10^{-6}	1.44×10^{-4}	-3.61×10^{-7}	0.9999156	1.161×10^{-5}
x_6	-1.06×10^{-6}	1.93×10^{-4}	-3.584×10^{-8}	0.9998324	1.151×10^{-5}
x_7	0.166×10^{-6}	-2.60×10^{-4}	-3.03×10^{-8}	0.9996730	1.133×10^{-5}
x_8	0.376×10^{-6}	1.36×10^{-4}	7.31×10^{-7}	0.9993642	1.096×10^{-5}
x_9	2.14×10^{-6}	-1.70×10^{-4}	-1.21×10^{-8}	0.9987724	1.027×10^{-5}
x_{10}	-1.43×10^{-6}	0.164×10^{-4}	-2.34×10^{-6}	0.9976857	0.899×10^{-5}
$f(x)$	7.66×10^{-6}	5.12×10^{-7}	7.21×10^{-6}	4.247×10^{-6}	1.25×10^{-9}

Table 10 Platform offset for original and optimised models

Offset of platform (m)		Offset of platform (% water depth)	
Original model	Optimised model	Original model	Optimised model
11.389	3.136	1.147	0.316

Table 11 Comparison of original and optimised mooring lines characteristics

Legend	Original model	Optimised model	Reduction (%)
Diameter (mm)	108.0	99.026	8.31
Wet weight (kN/m)	0.6007	0.5047	15.98
Length (m)	1828.7	1381.6	24.45
Fairlead slope (°)	45.89	51.347	NA
Pretension (kN)	2.312×10^3	2.0104×10^3	13.04

Table 12 Comparison of original and optimised mooring lines azimuth angles

Group	Mooring lines azimuth angles with respect to wave heading	
	Original model	Optimised model
I	45°, 50°	6.87°, 11.87°
II	125°, 132.5°	162.64°, 167.64°
III	222.3°, 229.7°, 235°	241.88°, 246.88°, 251.88°
IV	308.5°, 314.1°, 320.3°	303.30°, 308.30°, 313.30°

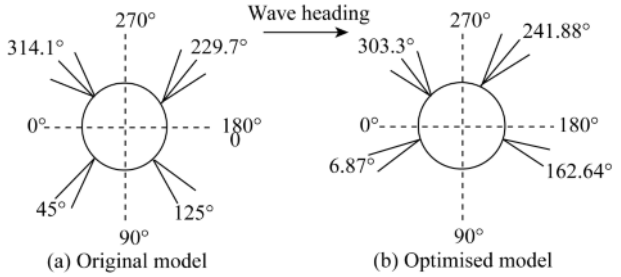

Fig. 18. Schematic diagram of original and optimised mooring systems.

(3) For both intact and damaged mooring conditions, the motions of platform exhibited at its new mean position for any line diameter, fairlead slope and pretension is nearly the same.

(4) Comparing the motions of platform about its new mean position between intact and damaged mooring conditions, revealed that the variation exhibited by any line diameter, fairlead slope and pretension is insignificant for all wave periods.

(5) For both intact and damaged mooring line conditions, the mean position attained by platform increases as with line diameter and decreases with increase in line fairlead slope/line pretension.

(6) Comparing the platform's new mean positions between intact and damaged mooring conditions, revealed that relatively higher variations are shown by larger line diameters, lower line pretensions and lower fairlead slopes.

Based on the study conducted with a truss spar platform subjected to the unidirectional wave, current and wind loadings – it is recommended to select the mooring configurations with line diameters below 127 mm (5″); line fairlead slopes from 50° to 65° and line pretension within 3.0×10^3 kN so that the dynamic responses of platform and effect of damaged condition is relatively small.

The optimising tool developed optimises the mooring configuration in terms of (a) Line azimuth angles; (b) Line diameter; (c) Line fairlead slope; and (d) Line pretension. This tool can economise the project cost by reduction in the analysis duration and manpower. Although the time taken by this tool varies with the environment and platform details, it can be concluded after demonstrating various cases that the optimum mooring configuration of truss spar platforms can be obtained within 60 minutes by one manpower against the trial and error approach which requires several days and a team of engineers.

The accuracy of the developed tool can be improved i.e. in terms of floater displacements and maximum line tensions by considering second order forces, mooring line dynamics, etc. The same will be investigated in the subsequent works.

Acknowledgment

This research was partially supported by YUTP-FRG funded by PETRONAS. We thank our colleagues who provided insight and expertise that greatly assisted the research.

References

Agarwal, A.K. and Jain, A.K., 2003. Dynamic behavior of offshore spar platforms under regular sea waves, *Ocean Engineering*, 30(4), 487–516.

Albrecht, C.H., 2005. *Algoritmos Evolutivos Aplicados À Síntese E Otimização de Sistemas de Ancoragem*, Ph.D. Thesis, Rio de Janeiro, RJ, Brasil.

Al-geelani, N.A., Piah, M.A.M., Adzis, Z. and Algeelani, M.A., 2013. Hybrid regrouping PSO based wavelet neural networks for characterization of acoustic signals due to surface discharges on H.V. glass insulators, *Applied Soft Computing*, 13(12), 4622–4632.

American Petroleum Institute, 2005. *Design and Analysis of Station-keeping Systems for Floating Structures*, API RP 2SK, API Publishing Services, Washington, USA.

Brits, R., Engelbrecht, A.P. and Van Den Bergh, F., 2002. A niching particle swarm optimizer, *Proceedings of the Fourth Asia-Pacific Conference on Simulated Evolution and Learning*, Singapore.

Cao, P.M., 1996. *Slow Motion Responses of Compliant Offshore Structures*, MSc. Thesis, Texas A&M University, Texas.

Chakrabarti, S.K., 1987. *Hydrodynamics of Offshore Structures*, Computational Mechanics Publications, Southampton.

Coello Coello, C.A., Luna, E.H. and Aguirre, A.H., 2003. Use of particle swarm optimization to design combinational logic circuits, *Proceedings of the International Conference on Evolvable Systems*: *From Biology to Hardware*, Springer, Trondheim, Norway, pp. 398–409.

Eberhart, R.C. and Shi, Y., 2000. Comparing inertia weights and constriction factors in particle swarm optimization, *Proceedings of the Congress on Evolutionary Computation*, IEEE, La Jolla, CA, USA, pp. 84–88.

Evers, G.I., 2009. *An Automatic Regrouping Mechanism to Deal with Stagnation in Particle Swarm Optimization*, MSc. Thesis, The University of Texas - Pan American, Edinburg, TX.

Glanville, R.S., Paulling, J.R., Halkyard, J.E. and Lehtinen, T.J., 1991. Analysis of the spar floating drilling production and storage structure, *Proceedings of the 23rd Offshore Technology Conference*, OTC, Houston, Texas.

Hassan, R., Cohanim, B., De Weck, O. and Venter, G., 2005. A comparison of particle swarm optimization and the genetic algorithm, *Proceedings of the 46th AIAA/ASME/ASCE/AHS/ASC Structures, Structural Dynamics and Materials Conference*, AIAA, Austin, Texas.

Horton, E.E. and Halkyard, J.E., 1992. A spar platform for developing deep water oil fields, *MTS'92*, Marine Technology Society, Washington, DC, USA, pp. 998–1005.

Hu, X.H., Eberhart, R.C. and Shi, Y.H., 2003. Engineering optimization with particle swarm, *Proceedings of 2003 IEEE Swarm Intelligence Symposium*, IEEE, Indianapolis, IN, USA, pp. 53–57.

Kathiravan, R. and Ganguli, R., 2007. Strength design of composite beam using gradient and particle swarm optimization, *Composite Structures*, (4), 471–479.

Kennedy, J. and Eberhart, R., 1995. Particle swarm optimization, *Proceedings of ICNN'95 - International Conference on Neural Networks*, IEEE, Perth, WA, Australia, pp. 1942–1948.

Krohling, R.A., dos Coelho, L.S. and Shi, Y.H., 2003. Cooperative particle swarm optimization for robust control system design, in: *Advances in Soft Computing: Engineering Design and Manufacturing*, Jose Manuel Benítez, Oscar Cordón, Frank Hoffmann, Rajkumar Roy (Eds.), Springer, London.

Magee, A.R., Sablok, A., Maher, J., Halkyard, J., Finn, L. and Datta, I., 2000. Heave plate effectiveness in the performance of truss spars, *Proceedings of the International Conference on Offshore Mechanics and Arctic Engineering*, New Orleans, pp. 469–479.

Mavrakos, S.A., Papazoglou, V.J., Triantafyllou, M.S. and Hatjigeorgiou, J., 1996. Deep water mooring dynamics, *Marine Structures*, 9(2), 181–209.

McCluskey, S., 2008. *Application of Particle Swarm Optimisation to Reinforced Concrete Beam Design*, Faculty of Engineering, UW.

Montasir, O.A., Yenduri, A. and Kurian, V.J., 2015. Effect of mooring line configurations on the dynamic responses of truss spar platforms, *Ocean Engineering*, 96, 161–172.

Montasir, O.A., Yenduri, A. and Kurian, V.J., 2016. Evaluation of the dynamic responses of truss spar platforms for various mooring configurations with damaged lines, *Ocean Engineering*, 123, 411–421.

Monteiro, B.F., Albrecht, C.H. and Jacob, B.P., 2010. Application of the particle swarm optimization method on the optimization of mooring systems for offshore oil exploitation, *Proceedings of the 2nd International Conference on Engineering Optimization*, Lisboa.

Pascoal, R., Huang, S., Barltrop, N. and Guedes Soares, C., 2005. Equivalent force model for the effect of mooring systems on the horizontal motions, *Applied Ocean Research*, 27(3), 165–172.

Pascoal, R., Huang, S., Barltrop, N. and Guedes Soares, C., 2006. Assessment of the effect of mooring systems on the horizontal motions with an equivalent force to model, *Ocean Engineering*, 33(11–12), 1644–1668.

Ran, Z.H., 2000. *Coupled Dynamic Analysis of Floating Structures in Waves and Currents*, Ph.D. Thesis, Texas A&M University, Texas, USA.

Shi, Y. and Eberhart, R., 1998. A modified particle swarm optimizer, *Proceedings of 1998 IEEE International Conference on Evolutionary Computation. IEEE World Congress on Computational Intelligence*, IEEE, Anchorage, AK, USA.

Smith, R.J. and MacFarlane, C.J., 2001. Statics of a three component mooring line, *Ocean Engineering*, 28(7), 899–914.

Technip document, 2005. *In Place Model Test Result Correlation*, Technip Marine (M) Sdn. Bhd, Malaysia.

Van Den Bergh, F. and Engelbrecht, A.P., 2001. Effects of swarm size on cooperative particle swarm optimisers, *Proceedings of the Genetic and Evolutionary Computation Conference*, San Francisco, USA.

Van Santen, J.A. and De Werk, K., 1976. On the typical qualities of spar type structures for initial or permanent field development, *Proceedings of the 8th Offshore Technology Conference*, OTC, Houston, Texas.

Wang, Z., 2012. *An Evolutionary Optimisation Study on Offshore Mooring System Design*, Ph.D. Thesis, University of Wollongong, Wollongong, Australia.

Yaakob, O., Zainudin, N., Samian, Y., Abdul, A.M., Malik, O.Y. and Palaraman, R.A., 2004. Developing Malaysian ocean wave database using satellite, *Proceedings of the 25th Asian Conference on Remote Sensing*, Geo-Informatics and Space Technology Development Agency, Chiang Mai, Thailand.

Zheng, Y.L., Ma, L.H., Zhang, L.Y. and Qian, J.X., 2003. Robust PID controller design using particle swarm optimizer, *Proceedings of 2003 IEEE International Symposium on Intelligent Control*, IEEE, Houston, TX, USA, pp. 974–979.